KU LEUVEN

WP EN2018-17

Optimal configuration for a low-temperature geothermal CHP plant based on thermoeconomic optimization

Sarah Van Erdeweghe, Johan Van Bael, Ben Laenen and William D'haeseleer

TME WORKING PAPER - Energy and Environment
Last update: April 2019

An electronic version of the paper may be downloaded from the TME website:
http://www.mech.kuleuven.be/tme/research/

KULeuven Energy Institute
TME Branch

Optimal configuration for a low-temperature geothermal CHP plant based on thermoeconomic optimization

Sarah Van Erdeweghe[a,c], Johan Van Bael[b,c], Ben Laenen[b], William D'haeseleer[a,c,*]

[a] *University of Leuven (KU Leuven), Applied Mechanics and Energy Conversion Section, Celestijnenlaan 300 - box 2421, B-3001 Leuven, Belgium*

[b] *Flemish Institute for Technological Research (VITO), Boeretang 200, B-2400 Mol, Belgium*

[c] *EnergyVille 1, Thor Park 8310, B-3600 Genk, Belgium*

Abstract

In this paper, we propose a thermoeconomic optimization procedure for four configurations of low-temperature geothermal combined heat-and-power (CHP) plants. The series, parallel, preheat-parallel and HB4 configurations are investigated. Electricity is produced via an organic Rankine cycle (ORC) and two types of district heating (DH) systems are considered for the heat delivery: a 90/60 and a 65/40 DH system. The objective is to maximize the net present value (NPV) of the CHP plant for given DH system requirements. We conclude that, under the assumptions considered, the NPV can be increased from -2.81MEUR (unprofitable) for a stand-alone electrical power plant to 12.5, 28 and 58MEUR (economically feasible) for the optimal CHP, and for a heat demand of 5, 10 and 20MWth, respectively. Also, the exergetic plant efficiency is higher for the CHP plants, which means that the geothermal energy source can be utilized in a better way. Furthermore, we have found that the series CHP is generally the optimal CHP configuration. Only for the 90/60 DH system and low heat demands, the HB4 is more suitable. Compared to the simple series and parallel CHPs, the HB4 configuration has a 16% and 5.5% higher NPV, for heat demands of 5 and 10MWth, respectively.

Keywords: geothermal energy, district heating, ORC, thermodynamic optimization, thermoeconomic optimization, CHP

*Corresponding author
Email address: william.dhaeseleer@kuleuven.be (William D'haeseleer)

1. Introduction

Geothermal energy is widely available all over the world. If one is willing to drill deep enough, this energy might be used for electrical power production. However in NW Europe, which is a non-volcanic region, geothermal electrical power plants are not economically feasible without some kind of financial support (e.g., a feed-in tariff) [1]. Therefore, in this paper, we try to improve the economic feasibility by providing heat in addition to electricity, in a combined heat-and-power (CHP) plant. We consider heat delivery to a nearby district heating (DH) system and electricity production via an organic Rankine cycle (ORC).

In the scientific literature, several studies have already been performed on the thermodynamic simulation or optimization of geothermal CHP plants connected to district heating systems [2, 3, 4, 5, 6, 7, 8]. A thermodynamic investigation of the simple series and parallel configurations has been performed in [2, 3, 4, 5]. Heberle et al. [2] have performed a thermodynamic simulation of the series and parallel configurations for a geothermal source temperature $T_{b,prod} = 80 - 150°C$ and flow rate of $150 m^3/h$. DH system temperatures of $T_{supply} = 75°C$ and $T_{return} = 50°C$ and a heat demand of $\dot{Q}_{DH} = 6.875 MW$ have been considered. They have concluded that the series configuration is the most efficient CHP set-up. Furthermore, they have concluded that ORC fluids with high critical temperatures like isopentane are favorable for a series CHP, whereas ORC fluids with low critical temperatures like R277ea are favorable for a parallel CHP or a stand-alone electrical power plant. Habka et al. [3] have studied the parallel and the so-called *Glewe* CHP set-ups for a geothermal source of $100°C$ and 1kg/s, for the connection to a district heating system with $T_{supply} = 60 - 90°C$ and $T_{return} = 40 - 55°C$. They have concluded that the electrical power output of the CHP is always lower than for a stand-alone power plant, and that it decreases with the heat demand of the DH system. However, the heat source utilization increases with the heat demand. Besides, they have concluded that the electrical power output of the parallel CHP is independent of the DH system supply temperature and that the electrical power output of the Glewe set-up decreases with T_{supply}. Finally, they have concluded that the Glewe configuration has no better performance than the simple series and parallel CHPs. In another paper, Habka et al. [4] have studied the series CHP for the same geothermal source and DH system conditions. They have found that the energetic and exergetic performance are improved for a lower return temperature, that the exergetic and energetic efficiencies increase with the heat demand and that there is an optimum for the exergetic efficiency

as a function of the supply temperature. Van Erdeweghe et al. [5] have also studied the series and parallel CHPs, using a standard and a recuperated ORC. We have considered a geothermal source of $130°C$ and 194kg/s, and the connection to a district heating system with $T_{supply} = 40 - 110°C$ and $T_{return} = 30 - 70°C$. We have concluded that the electrical power output is always equal to or lower than for the stand-alone electrical power plant, but that the heat source utilization is better. Furthermore, we have found that superheating might be beneficial for isentropic or dry working fluids in case of a constraint on the brine temperature at the ORC outlet.

Habka et al. have proposed some new CHP configurations in [6]. For similar source and DH system conditions as before, they have studied the series, parallel and four new CHP configurations, called *HB1* to *HB4*. The goal was to improve the electrical power output and heat source utilization with respect to the simple CHP set-ups. Based on the energetic and exergetic performance, its simplicity and flexibility, the authors have suggested that the HB4 configuration might become the state-of-the-art configuration for low-temperature geothermal CHP plants. For the investigated conditions, the HB4 configuration can produce up to 88% of the electrical power output of a stand-alone power plant. However, the authors did not include economics.

In follow-up work to [5], the authors of this paper have compared the series, parallel, preheat-parallel [9] and HB4 [6] configurations, based on the results of a thermodynamic optimization model with the electrical power output as the optimization objective in [7]. We have considered a 90/60 and a 65/40 DH system with heat demands of 5, 10 and 20MW. Geothermal source temperatures of $110 - 150°C$ and flow rates from $100 - 200$kg/s have been considered. We have concluded that the exergetic plant efficiency of the CHP is always higher than for a stand-alone electrical power plant. Furthermore, we have indicated the optimal configuration in all considered cases. Generally, the HB4 configuration as proposed in [6] has the highest electrical power output. Except for the 65/40 DH system at low brine flow rates and high heat demands, the series CHP performs better and for the 90/60 DH system, a low brine temperature and a low heat demand, the parallel CHP is more suitable. If there is a constraint on the brine injection temperature $T_{b,inj} \geq 70°C$, the series CHP is best for the 65/40 DH system. For the 90/60 DH system, the optimal configuration is similar to the case without constraint on the brine injection temperature.

Marty et al. [8] have studied the parallel CHP set-up for a geothermal source of $185°C$ and $350m^3$/h, and for the connection to a DH system with $T_{supply} = 95°C$ and $T_{return} = 65°C$. Like all

the thermodynamic studies before, they have assumed a fixed pinch-point-temperature difference, no pressure drop in the heat exchangers, fixed isentropic pump and turbine efficiencies. And additionally, they also assumed a fixed cooling water inlet temperature and fixed degrees of subcooling and superheating. However, they have included equipment cost models and optimized the net annual profit in their study. The main outcome of their work is a fast, robust and reliable optimization tool, and they have concluded that it is important to optimize the DH system configuration and the ORC size simultaneously.

Some additional thermodynamic studies [10, 11] are available which consider higher source temperatures. Oyewunmi et al. [10] have studied heat sources of 330, 250 and 150$^{\circ}C$ and heat delivery for hot water production. They have used the ORC condenser heat for heat delivery and concluded that the ORC exergetic efficiency increases with the hot water temperature. Furthermore, they have concluded that single-component fluids such as n-pentane are optimal for low-temperature heat demands and mixtures are optimal for high-temperature heat demands. Wieland et al. [11] have studied turbine-bleeding for heat delivery to a 80/50 DH system [1], and for source temperatures of 240 and 340$^{\circ}C$. They have concluded that the use of turbine-bleeding is optimal for high heat demands but that a parallel CHP performs better for low heat demands.

Finally, Fiaschi et al. [12] have studied the so-called *Cross-Parallel* configuration for a geothermal source of 130-170$^{\circ}C$ and 10kg/s. Industrial heat at higher temperatures (80-140$^{\circ}C$) is aimed at. They have concluded that, for the investigated conditions, up to 55% more electrical power can be produced compared to the parallel CHP. Furthermore, they have concluded that R227ea, R134a and R1234ze have the best performance for low heat demands and low heat utility temperatures whereas R245fa and n-butane have better performance for high heat demands and high utility temperatures.

From the literature study it follows that there are several thermodynamic studies available for geothermal CHP plants connected to DH systems. The main issues with these thermodynamic studies are the following: all cited papers make assumptions regarding the thermodynamic cycle parameters: fixed pinch-point-temperature differences, fixed isentropic efficiencies, no pressure drops in the heat exchangers, etc. In addition, simple thermodynamic models have been used, which

[1] A 80/50 DH system refers to a district heating system with $T_{supply} = 80^{\circ}C$ and $T_{supply} = 50^{\circ}C$.

do not account for the geometry (no use of friction factor and heat transfer coefficient correlations) and the size of the components. And finally, thermodynamic studies do not account for economics, so no conclusions can be drawn regarding the economic feasibility of the geothermal CHP plants. It should be mentioned, however, that Wieland et al. [11] have included an estimation for the revenues from selling electricity to the market. But no cost calculations or full economic analysis has been made.

As a consequence, the novelty of this paper is the thermoeconomic optimization and comparison of four low-temperature geothermal CHP plant configurations for the connection to two types of district heating systems. The conventional series and parallel CHP plants, the preheat-parallel CHP plant, which has been proposed by the authors in [9], and the HB4 CHP plant, which has been proposed and thermodynamically investigated by Habka et al. in [6], will be studied. The goal is to be able to indicate the best CHP configuration from a thermoeconomic point of view. Our optimization results are based on detailed thermodynamic models and proper economic costing models. Finally, we will also address the importance of taking economics into account by showing the difference with the simple thermodynamic optimization results.

2. Methodology

The methodology is based on the thermoeconomic design optimization procedure of geothermal power plants which has been developed in previous work [1]. We have expanded this methodology with the heat delivery to a district heating system for four different CHP configurations. Two types of district heating systems are considered. A high-temperature 90/60 DH system, for houses with a conventional heating system, and a low-temperature 65/40 DH system for houses with newer types of heating systems (e.g. floor heating).

2.1. Set-ups

Fig. 1 shows a schematic presentation of the four geothermal CHP configurations which are considered in this work. Besides the conventional series (S) and parallel (P) set-ups, we also study the preheat-parallel (PP) configuration [9] and the HB4 configuration [6].

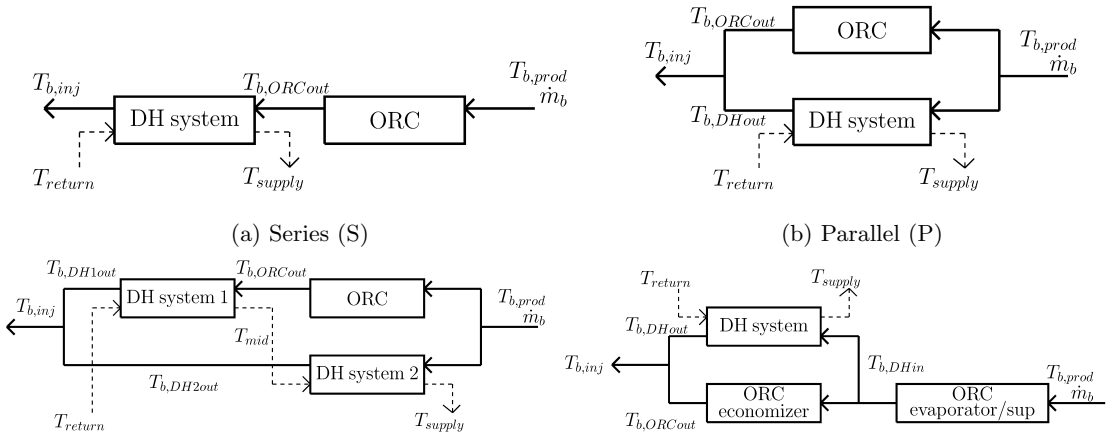

(a) Series (S)

(b) Parallel (P)

(c) Preheat-parallel (PP)

(d) HB4

Figure 1: CHP configurations with indication of the nomenclature. The full lines indicate the path of the brine (geothermal water) and the dashed lines indicate the path of the district heating system water.

For the electricity production, a standard and a recuperated ORC are investigated. Fig. 2a shows the set-up of a recuperated ORC.

The brine preheats, evaporates and superheats an ORC working fluid from state 3 → state 6. Then the ORC fluid expands in the turbine from state 6 → state 7, thereby delivering mechanical work which is converted to electricity via a generator. In case of a recuperator, the vapor at the turbine outlet (state 7 → state 8) is used to preheat the liquid after the pump (state 2 → 3), hence increasing the cycle efficiency. Then, the ORC fluid is condensed to a saturated liquid in state 1. And finally, the pump increases the pressure of the working fluid from state 1 → state 2. If no recuperator is used, state 2 = state 3 and state 7 = state 8. Fig. 2b shows the corresponding T-s diagrams for the standard (blue) and the recuperated (green) ORC. [2]

2.2. Reference parameter values

Table 1 summarizes the reference parameter values. The brine is modeled as pure water and the reference conditions (brine production temperature $T_{b,prod}$, pressure $p_{b,prod}$ and flow rate $\dot{m}_b$) are

[2]The T-s diagrams are the result of the thermoeconomic optimization model for a stand-alone electrical power plant [1], considering the reference parameter values of Table 1.

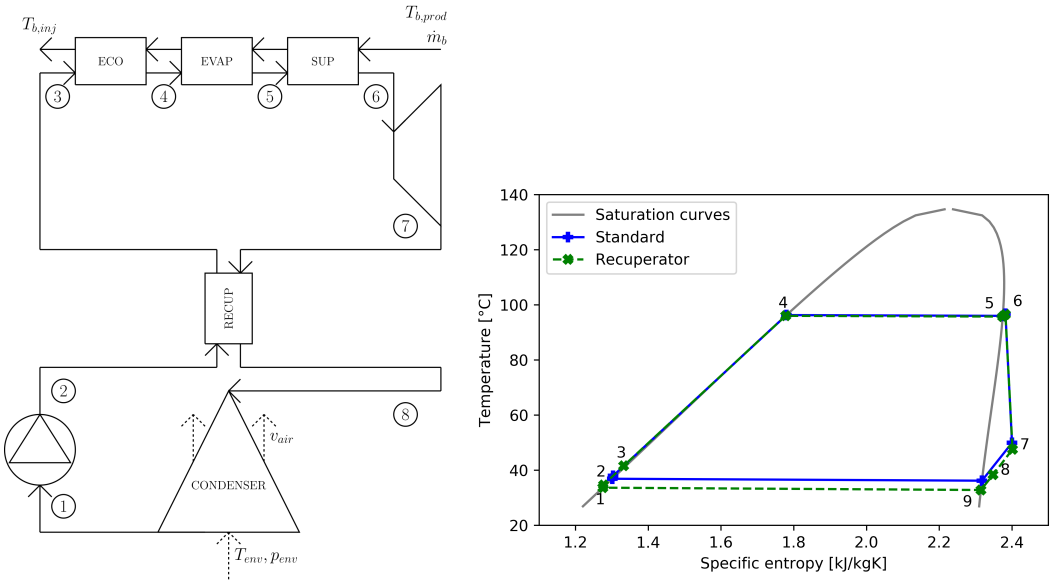

(a) Recuperated ORC.

(b) T-s diagram

Figure 2: Schematic presentation of the recuperated ORC and corresponding T-s diagram for the reference standard and recuperated cycle. For the standard ORC (without recuperator), state 2 = state 3 and state 7 = state 8.

Brine & wells	Economic	Environment	Cycle	DH system
$T_{b,prod} = 130°C$	$p_{el} = 60EUR/MWh$	$T_{env} = 10.85°C$	$\eta_p = 80\%$	T_{supply}
$p_{b,prod} = 40bar$	$d_{el} = 1.25\%/year$	$p_{env} = 1.02bar$	$\eta_g = 98\%$	T_{return}
$\dot{m}_b = 150kg/s$	$p_{heat} = 25EUR/MWh$		$\eta_m = 98\%$	$\dot{Q}_{DH}$
$I_{wells} = 15MEUR$	$dr = 5\%$		$\eta_f = 60\%$ [3]	$p_{supply} = 7bar$
$\dot{W}_{wells} = 500kW$	$L = 30years$		$\Delta T_{min} = 1°C$	
	$N = 90\%$		$\Delta T_{sup}^{min} = 1°C$	

Table 1: Reference parameter values.

taken from the Balmatt geothermal plant in Belgium [13]. Balmatt targets a fractured limestone reservoir at a depth of 3200-3600m. Reservoir pressure and temperature are characteristic for similar deep geothermal reservoir in NW Europe [14]. The well investment costs I_{wells} and well pumps power $\dot{W}_{wells}$ are also based on the preliminary results of the Balmatt geological site [13]. The constantly assumed electricity price p_{el}, yearly electricity price increase d_{el}, heat price p_{heat}, discount rate dr, lifetime L and availability factor N are the economic parameters. Furthermore, 2016 is taken as the reference year for all calculations. The reference environment conditions (T_{env}, p_{env}) are the average values for Mol in 2016 [15]. The cycle parameters are the pump isentropic efficiency η_p, the motor and generator efficiencies η_m and η_g, the fan efficiency η_f, the minimum pinch-point-temperature difference ΔT_{min} and the minimum degree of superheating ΔT_{sup}^{min}. The DH system parameters are the supply and return temperatures T_{supply} & T_{return}, the supply pressure p_{supply} and the heat demand $\dot{Q}_{DH}$. The reference values of the DH system operating temperatures are not given in Table 1 since two types of district heating systems are considered: $T_{supply} = 90°C$ & $T_{return} = 60°C$ or $T_{supply} = 65°C$ & $T_{return} = 40°C$. For each DH system, three values for the heat demand are studied: $\dot{Q}_{DH} = 5$, 10 or $20MWth$.

[3] $\eta_f = 60\%$ is the total fan efficiency, which includes the isentropic and mechanical-to-electrical conversion efficiency.

	mol. weight $[g/mole]$	T_{crit} $[°C]$	p_{crit} $[MPa]$	ODP	GWP
Isobutane (R600a)	58.12	134.66	3.63	0	20

Table 2: Thermodynamic and environmental properties of Isobutane (R600a) [17].

2.3. ORC fluid

Due to its good thermodynamic performance, the low cost of hydrocarbons [16] and its low environmental impact [17], we choose Isobutane as the ORC working fluid. The thermodynamic (molecular weight, and critical temperature and pressure) and environmental properties (ozone depletion potential, ODP, and global warming potential, GWP) are given in Table 2.

2.4. Optimization framework

First, the component choices and the thermoeconomic models are discussed. These detailed models are implemented in a thermoeconomic optimization model which calculates the optimal design of the CHP plants. The results of the thermoeconomic design optimization framework will be compared with the results of a purly thermodynamic optimization procedure. Therefore, we also shortly describe our thermodynamic optimization procedure, which has been presented in previous work [7].

2.4.1. Thermoeconomic models

We consider shell-and-tube TEMA E heat exchangers with a 30° tube layout [18]. For the economizer, evaporator and superheater, we assume the same geometry and the brine flows in the tubes, which eases the cleaning process. In case of a recuperator, the liquid flows through the tubes. An A-framed air-cooled condenser (ACC) with corrugated fins has been implemented. The legs of the A-frame make an angle of 60° with the horizontal, and the considered fins are vertically oriented in order to minimize fouling [19]. An axial turbine has been assumed, since it is commonly used in geothermal ORCs [20, 21]. Because of the small contribution of the ORC pump power and the ACC fan power to the ORC net power output, we consider constant values for the ORC pump efficiency and the ACC fan efficiency.

Detailed thermodynamic models for the friction factor, heat transfer coefficients and turbine efficiency calculation have been used, which we have described in our previous paper [1]. The bare equipment cost calculations are based on the heat transfer area for the heat exchangers and on the power for the ORC pump, turbine and ACC fans, and are also the same as in [1].

2.4.2. Thermoeconomic design optimization strategy

The goal of the thermoeconomic optimization procedure is to find the CHP design which corresponds to the highest net present value (NPV): [4]

$$
\begin{aligned}
max.\ & NPV \\
s.t.\ & 0 \leq D_{tube}/D_{shell} \leq 0.1 \\
& 0m \leq L_{ACC} \leq 15m \\
& \Delta T_{min}^{sup} \leq T_6 - T_4 \leq T_{upper} - T_{env} \\
& 10°C \leq T_4 - T_1 \leq 2\left(T_{upper} - T_{env}\right) \\
& T_{b,inj} \leq T_{b,prod} \\
& \Delta T_{min} \leq \Delta T_{pinch} \\
& \dot{Q}_{CHP} = \dot{Q}_{DH}
\end{aligned}
$$

The NPV is defined as:

$$
NPV = -I_{wells} - I_{ORC} - I_{DH} + \sum_{i=0}^{L-1} \frac{\left(\dot{W}_{net} p_{el} (1+d_{el})^i + \dot{Q}_{DH} p_{heat}\right) N 8760 - 0.025\left(I_{ORC} + I_{DH}\right)}{(1+dr)^i} \tag{1}
$$

[4] The so-called *payback period (PBP)* is not considered as an appropriate metric in Engineering Economics. The reason is that a customary PBP does not take into account a discount rate and furthermore it neglects the revenues obtained after the PBP. That is one of the reasons why net present value (NPV) is more appropriate for a given project duration. Alternatively, by setting the NPV equal to zero for a given project duration, one could compute the internal rate of return (IRR) for investors.

variable	lower bound	upper bound	variable	lower bound	upper bound
D_{shell} [m]	0.3	2	L_{bc} [m]	0.3	5
D_{tube} [mm]	5	50	S_{fin} [mm]	1.14	3.04
p_{tube}/D_{tube} [-]	1.2	2.5	H_{fin} [mm]	14.25	23.75
B_c/D_{shell} [-]	0.25	0.45	n_{tube} [-]	500	10000

Table 3: Bounds for the design variables in the optimization procedure, based on [19, 23].

Herein, we assume a yearly maintenance cost which is 2.5% of the ORC and DH heat exchanger(s) investment costs [22]. I_{ORC} and I_{DH} are the overnight installation costs for the ORC and the DH system heat exchanger(s), respectively. $\dot{W}_{net}$ and $\dot{Q}_{DH}$ are the net electrical power output and the heat production by the CHP.

The constraints on the tube-to-shell diameter ratio for the heat exchangers D_{tube}/D_{shell} and on the length of the air-cooled condenser legs L_{ACC} are imposed to ensure the validity of the correlations used. Furthermore, some operational constraints are set on the degree of superheating $T_6 - T_4$, on the difference between the evaporator and condenser temperature $T_4 - T_1$ (to have a proper cycle calculation), on the brine injection temperature $T_{b,inj}$ and on the pinch-point-temperature differences over the heat exchangers ΔT_{pinch}. T_{upper} is the maximal allowed temperature from the fluid properties database. The heat demand of the district heating system should be satisfied, which translates in the last constraint.

Table 3 summarizes the design variables. The bounds for the variables of the shell-and-tube heat exchangers (shell diameter D_{shell}, tube diameter D_{tube}, tube pitch p_{tube}, baffle cut length B_c and the length between the baffles L_{bc}) are based on the TEMA standards [23]. The bounds for the ACC design variables (fin height H_{fin}, fin spacing S_{fin} and the number of tubes n_{tubes}) are based on the validity of the correlations of Yang [19].

Besides the design variables, also some operating variables are optimized. These are the condenser temperature T_1, evaporator temperature T_4, turbine inlet temperature T_6, the ORC working fluid flow rate $\dot{m}_{wf}$, the air speed through the condenser v_{air} and the flow rate of the water in the DH system $\dot{m}_{DH}$. Depending on the use of a recuperator in the ORC, the recuperator efficiency ϵ ($= \frac{T_7 - T_8}{T_7 - T_2}$) is added. Depending on the CHP configuration, the brine flow rate to the DH system

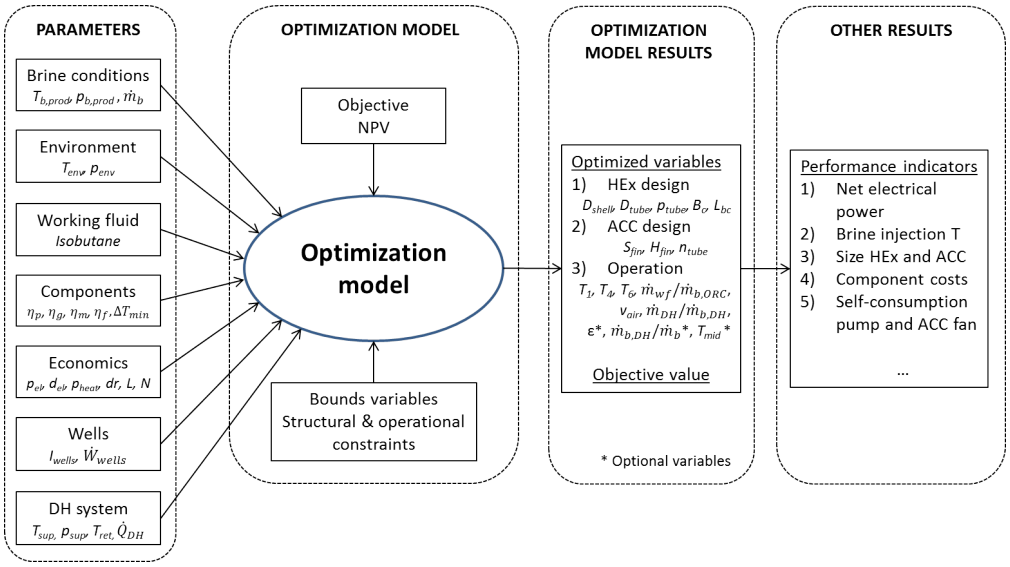

Figure 3: Flowchart of the thermoeconomic design optimization procedure.

branch $\dot{m}_{b,DH}$ (for the parallel, preheat-parallel and HB4 set-ups) and the intermediate temperature of the DH system water T_{mid} (for the preheat-parallel configuration) are added.

The flowchart of the CHP design optimization model is given in Fig. 3. A generic optimization methodology has been developed. All input parameters (regarding the brine, environment, economics, DH system, cycle and the working fluid) can easily be adapted. The NPV is chosen as the objective since it accounts for the thermodynamic performance, the size & cost of the components and the time value of money. The variable bounds and the structural and operational constraints are imposed to the optimization model. The results are the optimized ORC design and DH system heat exchanger design (optimal design variables of Table 3), the optimal values for the operating variables (temperatures and flow rates) and the value of the objective function. In a post-processing step, all other performance indicators can be calculated.

2.4.3. Thermodynamic cycle optimization strategy

In the simple thermodynamic optimization model, the net electrical power output $\dot{W}_{net}$ is considered as the optimization objective:

$$
\begin{aligned}
max.\ & \dot{W}_{net} \\
s.t.\ & \Delta T_{min}^{sup} \leq T_6 - T_4 \\
& 50°C \leq T_4 \leq T_{upper} \\
& T_{env} + 10°C \leq T_1 \leq 40°C \\
& T_{b,inj} \leq T_{b,prod} \\
& \Delta T_{min} \leq \Delta T_{pinch} \\
& \Delta T_{pinch}^{cond} = \Delta T_{pinch} \\
& \dot{Q}_{CHP} = \dot{Q}_{DH}
\end{aligned}
$$

Only constraints related to the thermodynamic cycle are imposed. In contrast to the thermoeconomic optimization procedure, detailed correlations for heat transfer coefficients and friction factors are not used here, but simple input-output models are used. Also the pressure drop in the heat exchangers is neglected. The geometry and size of the components is not modeled (therefore no structural constraints are imposed here) and no economics are considered in the thermodynamic optimization procedure.

The variables are the operating temperatures and flow rates. In contrast to our previous study [7], where we have considered R236ea as the ORC working fluid, we consider Isobutane since it is less harmful to the environment compared to R236ea.

The parameter values related to the brine & wells, the environment and the DH system are the same as in Table 1. However, the economic parameters are not included in this thermo*dynamic* model and some of the cycle parameters are different. For the cycle parameters: a minimal temperature difference over the heat exchangers of $\Delta T_{min} = 5°C$, a minimal degree of superheating of $\Delta T_{min}^{sup} = 0.01°C$ and a turbine isentropic efficiency of 88.5% are assumed. The values for η_p, η_g and η_m are the same as in Table 1. In addition, a direct water cooled condenser [5] is considered for the

[5] In the thermodynamic optimization procedure, the electrical power output — which is the optimization objective — does not depend on the type of cooling system. The condenser pressure (of the ORC working fluid) determines

thermodynamic optimization, and the following cooling water inlet conditions are assumed: $T_{cw} = 12°C$ and $p_{cw} = 2bar$.

2.4.4. Implementation

All models are implemented in Python [24], using the CasADi [25] optimization framework and the IpOpt [26] non-linear solver. The fluid properties are called from the REFPROP database [27].

3. Results

First, some performance indicators are defined. Then, the results of the thermoeconomic design optimization model are given for the four CHP configurations and for two types of district heating systems. Afterwards, the results are compared with the results of a purely thermodynamic optimization and a summary of the main conclusions is given.

3.1. Definition of the performance indicators

Some performance indicators are used to indicate how good a CHP configuration operates. The Net Present Value (NPV) was already explained in Section 2.4.2. Other performance indicators which we will use in this paper are:

- the net electrical power output $\dot{W}_{net}$;
- the ORC overnight installation cost I_{ORC};
- the heat exchangers installation cost for the connection of the DH system I_{DH};
- the energetic cycle efficiency $\eta_{en} = \frac{\dot{W}_t - \dot{W}_p}{\dot{Q}_b}$
  with $\dot{Q}_b = \dot{m}_b(h_{b,prod} - h_{b,ORCout})$;
- the exergetic plant efficiency

$$\eta_{ex} = \frac{\dot{W}_{net} + \dot{E}x_{DH}}{\dot{E}x_{b,prod}} \tag{2}$$

the electricity production.

with $\dot{E}x_{b,prod} = \dot{m}_b ex_{b,prod}$
and $ex = h - h_{env} - T_{env}(s - s_{env})$.

3.2. Thermoeconomic design optimization results

The main goal is to find the best CHP configuration and its optimal design, for the connection to a certain type of district heating system and heat demand. A 90/60 and a 65/40 DH system are considered with a heat demand of 5, 10 and 20MWth. The four CHP configurations of Fig. 1 with implementation of a recuperated and a standard ORC are studied.

3.2.1. Recuperated ORC versus standard cycle

For the connection to a 65/40 DH system, all CHP configurations with a recuperated ORC have a 8%, 3% and $1-2$% higher NPV than the implementation with a standard ORC for a heat demand of 5, 10 and 20 MWth, respectively. For the connection to a 90/60 DH system, the parallel, preheat-parallel and HB4 configurations have a $8-9$%, $3-4$% and $1-2$% higher NPV with a recuperated cycle compared to the implementation with a standard ORC. For the series CHP, these values are 15%, 6% and 3%. The influence of the heat demand will be discussed further on (in Fig. 4). For the series CHP, the difference between the recuperated and the standard ORC is more outspoken due to the big impact of the DH system temperatures on the brine temperature at the ORC outlet. $T_{b,ORCout}$ is always higher for the recuperated cycle than for the standard ORC (due to the recuperator), which makes the recuperated ORC more suitable for the series CHP connected to a high-temperature DH system. So, we can conclude that for all considered cases, the use of a recuperated ORC results in a higher NPV than the implementation of a standard ORC.

3.2.2. Combined heat-and-power plant configurations

Fig. 4 shows the NPV for all four CHP configurations for the two types of district heating systems, and as a function of the heat demand. The results for a recuperated ORC are shown since these have the highest NPV. For comparison, the recuperated ORC as a stand-alone electrical power plant is given in gray (no heat demand: $\dot{Q}_{DH} = 0$). The series, parallel, preheat-parallel and HB4 CHP configurations are shown in blue, green, red and magenta, respectively. This color code will be

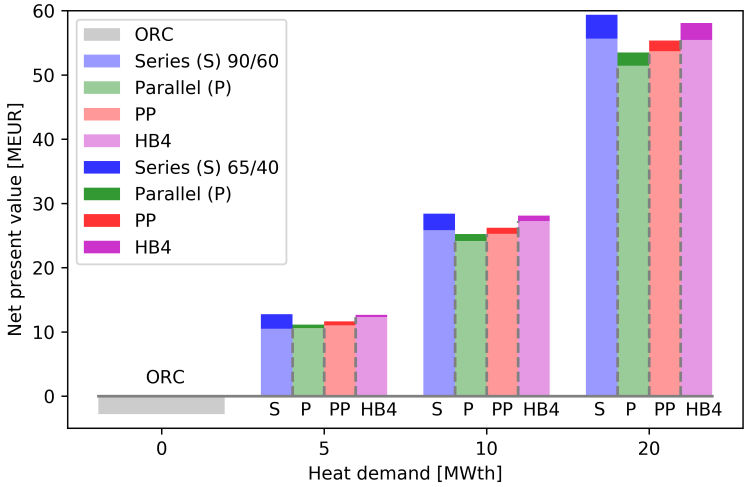

Figure 4: Net present value (NPV) of the recuperated CHP configurations as a function of the DH system heat demand, and for the connection to a 65/40 (opaque) and a 90/60 (more transparent) district heating system. The letters *S*, *P*, *PP* and *HB4* indicate the bars with results for the series (blue), the parallel (green), the preheat-parallel (ref) and the HB4 (magenta) CHP configurations, respectively. *ORC* indicates the stand-alone electrical power plant (gray). For a good presentation of the color figure, the reader is kindly referred to the online version of this paper.

used throughout the entire paper. The opaque bars indicate the connection to a 65/40 DH system, the more transparent bars represent the connection to a 90/60 DH system.

From Fig. 4 it follows that all CHP configurations have a higher NPV than the stand-alone electrical power plant, and the NPV increases nearly linearly with the heat demand. So we might enhance the economic profitability by providing heat next to electricity. Furthermore, for each DH system type and heat demand, we can indicate the most suitable CHP configuration. The series CHP is the optimal configuration for the connection to a 65/40 DH system. However, for the 90/60 DH system, the HB4 configuration is more suitable for a heat demand of 5 and 10MWth. Compared to the simple CHP configurations, the HB4 CHP has a 16% higher NPV for the 5MWth 90/60 DH system case (compared to the parallel CHP which would be optimal) and a 5.5% higher NPV for the 10MWth 90/60 DH system case (compared to the series CHP which would be optimal). The preheat-parallel configuration is never optimal but performs better than the simple series and parallel CHPs for the 5MWth 90/60 DH system case, with a 4% higher NPV.

Fig. 5 shows three more performance indicators: the net electrical power output $\dot{W}_{net}$, the exergetic plant efficiency η_{ex} and the energetic ORC cycle effciency η_{en}. In addition, three operating temperatures are shown: the brine injection temperature $T_{b,inj}$, the brine temperature at the ORC outlet $T_{b,ORCout}$ and at the DH system outlet $T_{b,DHout}$. For now, we only consider the thermoeconomic results (colored bars). The thermodynamic optimization results (indicated by the black lines and hatches) will be discussed in Section 3.3.2.

The ranking for the CHPs with the highest electrical power output is the same as the ranking based on the NPV. We see on Fig. 5a that the series and HB4 CHP configurations are able to keep a high net electrical power output for a higher heat demand of the DH system. The electrical power output of the series CHP decreases less fast with the DH system heat demand compared to the HB4 configuration. Therefore, the series CHP is recommended for very high heat demands, and the HB4 for moderate heat demands. The parallel configuration is most suitable for low heat demands of the DH system, but has a low electricity production for high heat demands due to the lower brine flow rate to the ORC branch. The preheat-parallel configuration does not give significant improvements compared to the conventional CHPs, and is always outperformed by the HB4 configuration. Also, as expected, Fig. 5a shows that the CHP configurations have a lower electrical power output than the stand-alone electrical power plant.

Fig. 5b shows the exergetic plant efficiency for all configurations. As for $\dot{W}_{net}$, the ranking for the CHPs with the highest η_{ex} is the same as the ranking based on the NPV. Note that all CHPs have a higher value of η_{ex} than the stand-alone electrical power plant. The exergetic plant efficiency is directly related to the heat source utilization, which means that the low-temperature geothermal energy source is utilized better in a CHP plant than in a stand-alone electrical power plant. Furthermore, from Fig. 5b it follows that the exergetic plant efficiency is mostly higher for the connection to a 90/60 DH system, despite a lower electricity production, compared to the 65/40 DH system case. This is due to the higher exergetic value of the same amount of thermal energy. The only exception is the series CHP at low heat demands. For a heat demand of 5 and 10MWth, η_{ex} for the connection with a 90/60 DH system is respectively 3.03%-pts and 0.82%-pts lower than for the connection to a 65/40 DH system. In this case the impact of a lower electrical power production $\dot{W}_{net}$ is bigger than the beneficial effect of a higher exergy content of the heat (see Eq. (2) for the definition of η_{ex}).

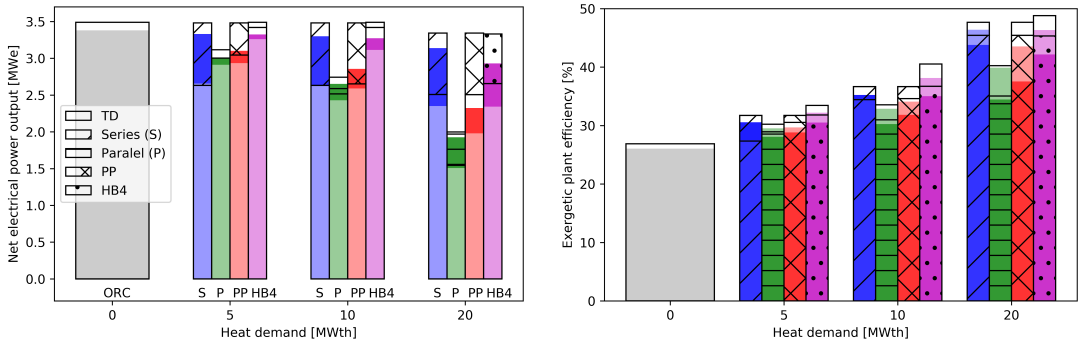

(a) $\dot{W}_{net}$ (b) η_{ex}

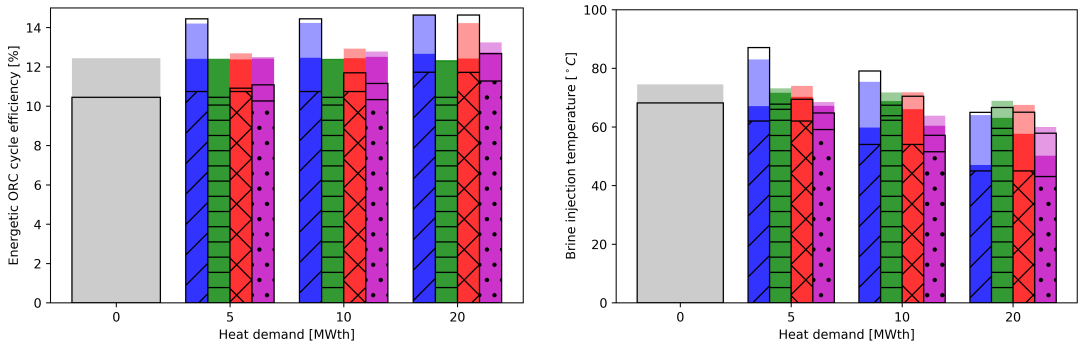

(c) η_{en} (d) $T_{b,inj}$

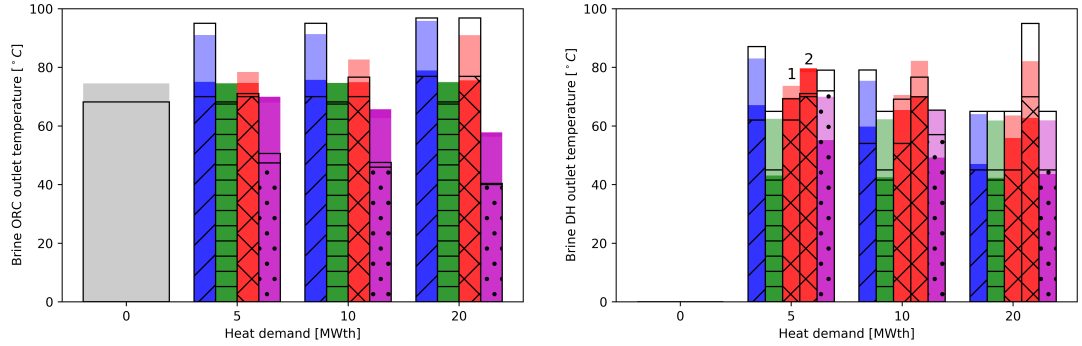

(e) $T_{b,ORCout}$ (f) $T_{b,DHout}$

Figure 5: Comparison of the thermoeconomic (TE) and the thermodynamic (TD) optimization results, for the recuperated ORC and the CHP plant configurations (with a recuperated ORC). The TE optimization results are indicated by the colored bars (same color code as in Fig. 4). The TD optimization results are indicated by the black empty bars, using hatches for the connection to a 65/40 DH system and no fill for the 90/60 DH system results. For a good presentation of the color figure, the reader is kindly referred to the online version of this paper.

Fig. 5c shows the energetic cycle efficiency for all CHP configurations. For the 65/40 DH system, the HB4 CHP has the highest η_{en}, followed by the series CHP. The preheat-parallel configuration tends more towards a series CHP for high heat demands and for the connection to a low-temperature DH system, which explains the trend of η_{en}. For the connection to a 90/60 DH system, the series CHP has the highest η_{en} due to the constraint on the ORC outlet temperature $T_{b,ORCout}$. The series CHP is followed by the preheat-parallel CHP (which is also sensitive to high values of $T_{b,ORCout}$), the HB4 configuration and the parallel set-up. For all CHPs, the value of η_{en} is higher for the connection to a 90/60 DH system than for a 65/40 DH system. Except for the parallel CHP, η_{en} is independent of the DH system temperatures.

The brine injection temperature is given in Fig. 5d. For all CHPs, the value of $T_{b,inj}$ is higher for the connection to a DH system with higher operating temperatures, which is logical. For the 65/40 DH system, $T_{b,inj}$ is the highest for the parallel CHP, followed by the preheat-parallel, HB4 and series CHPs. For the 90/60 DH system, the series CHP has the highest value of $T_{b,inj}$, followed by the preheat-parallel, the parallel and the HB4 CHPs for low heat demands. For a heat demand of 20MWth, the parallel CHP has the highest injection temperature, followed by the preheat-parallel CHP, the series CHP and the HB4 configuration. A big advantage of the HB4 configuration is the ability to cool down the brine much further than the other configurations for high-temperature district heating systems. The lower the value of $T_{b,inj}$, the more energy is extracted from the geothermal energy source. The brine injection temperature and the energetic cycle efficiency are the two main contributions to the exergetic plant efficiency η_{ex}.

The brine temperature at the outlet of the ORC is given in Fig. 5e. For the parallel CHP set-up, the value of $T_{b,ORCout}$ is almost independent of the heat demand (slightly increasing for higher heat demands and for higher temperatures of the DH system).[6] The value of $T_{b,ORCout}$ for the series CHP depends strongly on the district heating system temperatures. Also for the preheat-parallel configuration, $T_{b,ORCout}$ depends (to a lesser extent) on the DH operating temperatures. For the HB4 configuration, however, the ORC outlet temperature is lower in case of higher temperatures of the DH system. For high temperatures of the DH system, more brine flow rate is needed in the

[6]For higher values of the heat demand and for the district heating system temperatures, less heat of the brine can be fed to the ORC and a cheaper ORC will be installed. This cheaper ORC is less efficient and less energy will be extracted from the brine, which results in a higher value of $T_{b,ORCout}$.

DH system branch and less brine flow rate is available for the economizer of the ORC. Therefore, by lowering the brine temperature at the economizer outlet, more heat can be extracted from the brine to keep an as high as possible electricity production. Similarly, for higher heat demands the ORC outlet temperature decreases.

Finally, Fig. 5f shows the brine temperature at the outlet of the DH system heat exchanger(s). Since the preheat-parallel configuration has two heat exchangers which are connected with the DH system, this configuration has two bars in Fig. 5f. *1* and *2* refer to the first and second DH system heat exchanger, following the nomenclature of Fig. 1. In general, the value of $T_{b,DHout}$ decreases with the heat demand and is higher for the connection to a DH system with higher operating temperature. For the parallel CHP, the value of $T_{b,DHout}$ is almost constant as a function of the heat demand. For the series CHP, the value of $T_{b,DHout}$ strongly decreases with the heat demand (until the minimal pinch-point-temperature difference is reached at the brine outlet side). Similar trends hold for the HB4 CHP, but these are less outspoken. For the preheat-parallel configuration and the connection to the 65/40 DH system, the trends are similar to the series CHP. However, for the connection to the 90/60 DH system, *DH HEx 1* (following the nomenclature of Fig. 1) follows the trend for the series CHP whereas *DH HEx 2* follows the trend for a parallel CHP.

3.2.3. Optimal configuration

Table 4 shows the performance indicators for the optimal CHP configuration, for the connection to a 90/60 and a 65/40 DH system and for different heat demands. For comparison reasons, also the performance of a stand-alone electrical power plant is shown ($\dot{Q}_{DH} = 0MWth$). For the 65/40 DH system, the series CHP with recuperated ORC is the most suitable configuration. Also for the 90/60 DH system and a high heat demand of $\dot{Q}_{DH} = 20MWth$, the series CHP has the highest NPV. However, for heat demands of $\dot{Q}_{DH} = 5$ and $10MWth$, the HB4 configuration is more favorable.

In general, the NPV increases with the heat demand, and is higher for the connection to a low-temperature DH system. Also note that by providing heat next to electricity, the geothermal project goes from an economically infeasible project ($NPV < 0$ for the stand-alone electrical power plant) to an economically attractive project ($NPV > 0$). So, the economic attractiveness of a geothermal project can be enhanced by providing heat in addition to electricity. However, the net electrical

$\dot{\mathbf{Q}}_{\mathbf{DH}} = \mathbf{0MWth}$		$\dot{\mathbf{Q}}_{\mathbf{DH}} = \mathbf{5MWth}$	$\dot{\mathbf{Q}}_{\mathbf{DH}} = \mathbf{10MWth}$	$\dot{\mathbf{Q}}_{\mathbf{DH}} = \mathbf{20MWth}$
ORC	**65/40 DH system**	**Series**	**Series**	**Series**
$NPV = -2.81MEUR$		$NPV = 12.76MEUR$	$NPV = 28.41MEUR$	$NPV = 59.37MEUR$
$\dot{W}_{net} = 3.38MWe$		$\dot{W}_{net} = 3.33MWe$	$\dot{W}_{net} = 3.30MWe$	$\dot{W}_{net} = 3.14MWe$
$I_{ORC} = 12.49MEUR$		$I_{ORC} = 12.22MEUR$	$I_{ORC} = 12.06MEUR$	$I_{ORC} = 11.24MEUR$
$I_{DH} = 0.00MEUR$		$I_{DH} = 0.20MEUR$	$I_{DH} = 0.35MEUR$	$I_{DH} = 0.77MEUR$
$\eta_{ex} = 26.05\%$		$\eta_{ex} = 30.58\%$	$\eta_{ex} = 35.24\%$	$\eta_{ex} = 43.81\%$
$T_{b,inj} = 74.52°C$		$T_{b,inj} = 67.09°C$	$T_{b,inj} = 59.79°C$	$T_{b,inj} = 47.03°C$
	90/60 DH system	**HB4**	**HB4**	**Series**
		$NPV = 12.30MEUR$	$NPV = 27.25MEUR$	$NPV = 55.65MEUR$
		$\dot{W}_{net} = 3.26MWe$	$\dot{W}_{net} = 3.11MWe$	$\dot{W}_{net} = 2.35MWe$
		$I_{ORC} = 12.03MEUR$	$I_{ORC} = 11.54MEUR$	$I_{ORC} = 8.48MEUR$
		$I_{DH} = 0.29MEUR$	$I_{DH} = 0.54MEUR$	$I_{DH} = 1.26MEUR$
		$\eta_{ex} = 32.21\%$	$\eta_{ex} = 38.14\%$	$\eta_{ex} = 46.41\%$
		$T_{b,inj} = 68.53°C$	$T_{b,inj} = 63.81°C$	$T_{b,inj} = 64.02°C$

Table 4: Performance indicators for the optimal CHP configuration, for the connection to a 65/40 and a 90/60 DH system and for different heat demands. For comparison, also the results for a stand-alone electrical power plant are shown. All configurations have a recuperated ORC.

power output decreases with the heat demand. For $\dot{Q}_{DH} = 20MWth$ and the connection to a 65/40 DH system, the net electrical power production is still 93% of the stand-alone electrical power plant. However, for the connection to a 90/60 DH system, this value drops to 70%. The exergetic plant efficiency increases with the heat demand, and more for heat delivery at higher temperatures due to the higher exergetic value of the same energy content of heat. Compared to the stand-alone power plant, the exergetic plant efficiency can be increased with 17.76%-pts and 20.36%-pts for a heat demand of 20MWth and for the connection to a 65/40 and a 90/60 DH system, respectively. This indicates a better utilization of the geothermal source in the CHP plants than in a stand-alone electrical power plant. Due to the better brine utilization, the injection temperature is lower for the CHP plants than for the stand-alone electrical power plant. The ORC investment cost (and the ORC efficiency) drops for a higher heat demand. Since the electrical power output is lower for higher heat demands, there is no incentive to invest in a more expensive ORC. This effect is the strongest for the connection to a high-temperature DH system. Also the investment costs for the heat exchanger(s) for heat delivery are higher for the connection to a high-temperature DH system.

3.3. Comparison with pure thermodynamic optimization results

In this section, we compare the results of our detailed thermoeconomic optimization model for the four CHP configurations of Fig. 1 with the results of a simple thermodynamic optimization model.

3.3.1. Stand-alone electrical power plant

Fig. 6a shows the T-s diagrams of the recuperated ORC, which is optimized by the thermodynamic (TD) model in full lines and which is optimized by the thermoeconomic (TE) model in dashed lines. Only the results for the recuperated cycle are shown.[7] From the T-s diagram is clear that all operating temperatures are lower in case of the TD optimized results. This is a direct consequence of the different cooling temperatures and the different minimal pinch-point-temperature difference.

[7]The T-s diagrams of the recuperated and the standard ORC cycle look similar. The condenser temperature is the lower limit as set in the TD optimization procedure: $T_1 = T_{env} + 10°C$, the evaporator and turbine inlet temperatures are slightly higher for the standard ORC ($\approx 0.71°C$).

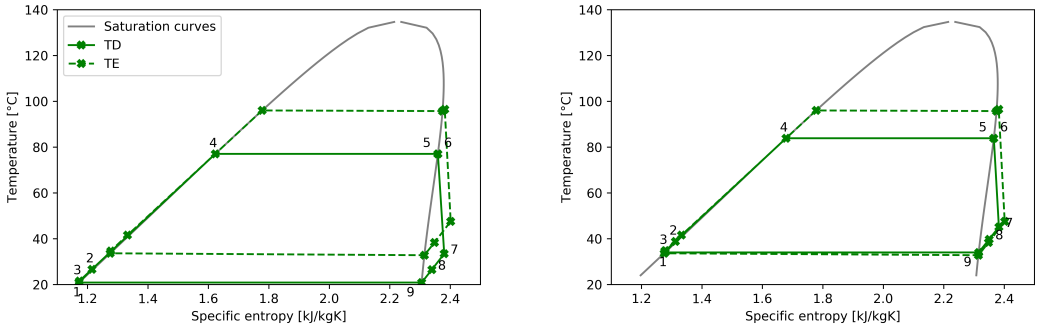

(a) Reference parameters

(b) $T_{cond} = 34°C$ for TD optimization

Figure 6: T-s diagrams of the optimized recuperated ORC. The results of the thermodynamic (TD) optimization are indicated by the full lines, the results of the thermoeconomic (TE) optimization by the dashed lines. The T-s diagram of the TE optimization results is the same in both figures.

The lower limit on the condenser temperature for the TD optimization is $T_1 = T_{env} + 10°C = 20.85°C$, whereas for the TE optimization T_1 is optimized and is approximately $34°C$. In the thermoeconomic optimization procedure, the size and cost of the cooling system are taken into account (a lower condenser temperature would result in a bigger and more expensive cooling system) whereas the lower limit for T_1 sets the condenser temperature in the thermodynamic optimization model (highest electricity production, costs are not considered). Because of the big impact of the condenser temperature, we try to improve this parameter assumption in the TD optimization model. We set $T_1^{min} = 37$ and $34°C$ for the standard and the recuperated ORC, respectively. These values are very close to the TE optimized values. Fig. 6b shows the new T-s diagram. The condenser temperature is very close, but still the evaporator temperature of the TD optimization results is lower than the TE optimized value. This is because in the TD optimization procedure, we assume a minimum temperature difference $\Delta T_{min} = 5°C$, whereas in the TE optimization procedure $\Delta T_{min} = 1°C$. Furthermore, the main driver for the difference in evaporator temperature is the fact that we do not account for the component size and cost in the TD optimization procedure. From a cost-perspective, it is beneficial to increase the evaporator temperature and decrease the ORC fluid mass flow rate.

Table 5 shows more detailed results for the TD and TE optimization of a stand-alone geothermal

	standard			recuperator		
	TE	TD		TE	TD	
$\dot{W}_{net}$ [MWe]	3.11	3.18	4.92	3.38	3.49	4.92
η_{en} [%]	11.45	9.78	11.79	12.44	10.45	12.06
η_{ex} [%]	23.99	24.65	37.94	26.05	26.89	37.93
$T_{b,inj}$ [$°C$]	73.53	68.73	55.44	74.52	68.18	57.15
T_6 [$°C$]	96.76	85.03	77.76	96.51	83.87	77.05
T_4 [$°C$]	95.76	85.02	77.75	95.51	83.86	77.04
T_1 [$°C$]	36.87	**37.00**	**20.85**	33.63	**34.00**	**20.85**
$\dot{m}_{wf}$ [kg/s]	92.83	104.06	116.47	93.48	106.09	117.64
ϵ [%]	-	-	-	71.15	51.76	58.08

Table 5: Comparison of the thermoeconomic (TE) and the thermodynamic (TD) optimization results for the standard and the recuperated ORC.

power plant. Since the condenser temperatures $T_1^{min} = 37$ and $34°C$ for the standard and the recuperated ORC, are closer to the thermoeconomic optimization results, it is a better base for comparison and we will use the first column of the TD results in Table 5. The following conclusions are made:

- The electrical power output is slightly overestimated by the TD model results in comparison to the TE model: with 2.89% and 3.25% for the standard and the recuperated cycle, respectively. The higher electricity production is the result of a lower evaporator temperature T_4 and a higher ORC fluid flow rate $\dot{m}_{wf}$.
- The exergetic plant efficiency is directly related with the electrical power output in case of a stand-alone power plant. As a consequence, also the exergetic plant efficiency is overestimated by 2.89% and 3.25% or by 0.66%-pts and 0.84%-pts, for the standard and the recuperated ORC.
- Since the electrical power output is optimized in the TD optimization procedure, the energetic cycle efficiency does not really matter. In the TE optimization results, the energetic efficiency is related to the compactness, size and cost of the ORC. Therefore, η_{en} is higher for the TE optimization model results.

- The brine injection temperature is lower for the TD optimization results. When we account for the size and cost (in the TE model), using the brine until a lower temperature means that a larger and more costly heat exchanger is needed.
- Since the expansion from a higher turbine inlet temperature results in a higher degree of superheating of the turbine exit vapor, the recuperator efficiency is higher in case of the thermoeconomic optimization results.

If we would compare the TE optimization results with the TD results based on the reference condenser temperature of $T_1 = 20.85°C$, which we have used before [7], the trends are similar but more outspoken. In addition, the cooling system cost (which is ∼70% of the total ORC investment costs) is very important but is not accounted for in the thermodynamic optimization model results.

3.3.2. Combined heat-and-power plant configurations

We refer to Fig. 5, which also shows the thermodynamic optimization results for the recuperated CHP configurations. The bars are empty for the 90/60 DH system and are filled with hatches for the 65/40 DH system. The first bar shows the thermodynamic optimization result for the recuperated stand-alone electrical power plant.

For the connection to a 90/60 DH system, the HB4 configuration has by far the highest electrical power output. $\dot{W}_{net}$ is 12.31%, 28.92% and 5.96% higher than the preheat-parallel configuration. For low heat demands, the series CHP has the lowest electrical power output whereas the parallel CHP has the lowest power output for high heat demands due to the smaller brine flow rate which is available for the ORC. For the connection to a 65/40 DH system, the series and the HB4 CHPs have the highest electrical power output. The differences in $\dot{W}_{net}$ are negligible ($< 0.4\%$). The preheat-parallel CHP operates as a series configuration. The parallel CHP is significantly less-performing due to the lower brine flow rate which goes to the ORC. We can see from Fig. 5 that the electrical power output which is predicted by the TD optimization results (black) is higher than $\dot{W}_{net}$ which was calculated by the TE optimization model (colored bars).

The exergetic plant efficiency is probably the most useful indicator to investigate the thermodynamic performance of the CHP configurations. As for the TE optimization results, in most cases η_{ex} for

the connection to the 90/60 DH system is higher than for the 65/40 DH system connection. As for the TE results, the series CHP for low values of the heat demand is an exception. In contrast to the TE optimization results, η_{ex} for the preheat-parallel configuration and for heat demands of 5 and 10MWth is 1.19%-pts and 2.05%-pts higher for the connection to a 65/40 DH system than for the 90/60 DH system. As a direct result of the overestimated electrical power production by the TD model, also the exergetic plant efficiency is overestimated compared to the TE optimization results.

As for the stand-alone electrical power plant (Section 3.3.1), the energetic ORC cycle efficiency is underestimated by the TD optimization model. However, for the connection to a high-temperature DH system, the series CHP and for high heat demands also the preheat-parallel CHP show higher η_{en} for the TD results than for the TE results. This is mainly due to the different minimal temperature assumption over the heat exchanger: $\Delta T_{min} = 1°C$ for the TE optimization model and $\Delta T_{min} = 5°C$ for the TD optimization model. As a result, for these cases, the ORC outlet temperature of the brine ($T_{b,ORCout}$, see Fig. 5e) is higher for the TD results than for the TE results. This also causes a higher value of η_{en}. Also due to the same reason, the brine injection temperature of the series CHP connected with a 90/60 DH system is higher for the TD optimization results than for the TE results. The other CHP configurations follow the trends of the stand-alone electrical power plant as explained in Section 3.3.1.

Finally, the trends for the brine temperature at the DH system heat exchanger outlet ($T_{b,DHout}$, Fig. 5f) are strongly related to the difference in ΔT_{min}. For high heat demands, the minimal temperature difference is reached at the brine outlet side of the DH system heat exchanger. Since $\Delta T_{min} = 1°C$ for the TE optimization model and $\Delta T_{min} = 5°C$ for the TD optimization model, the TE optimized schemes might go to a lower value of $T_{b,DHout}$

3.4. Summary

Table 6 gives the ranking of the CHPs and the stand-alone electrical power plant, all with the implementation of a recuperated ORC, based on the thermoeconomic results on the one hand, and on the simple thermodynamic optimization results on the other hand. The first column shows the *real* ranking based on the NPV, using the results of the detailed thermoeconomic optimization model. Columns 2 and 3 give the ranking based on the corresponding electrical power output from

the thermoeconomic optimization model and the ranking for $\dot{W}_{net}$ based on the simple thermodynamic optimization model results, respectively. Columns 4 and 5 show the analogue results for the exergetic plant efficiency.

First, the rankings of the CHP configurations based on the thermoeconomic (TE) optimization model results (with NPV as the optimization objective) for the NPV, $\dot{W}_{ex}$ and η_{ex} are the same. Second, also the rankings of the CHP configurations based on the thermodynamic (TD) optimization results (with $\dot{W}_{net}$ as the optimization objective) for $\dot{W}_{ex}$ and η_{ex} are the same. The fact that the rankings for $\dot{W}_{ex}$ and η_{ex} are the same is expected since η_{ex} directly depends on $\dot{W}_{net}$ for a fixed heat demand and DH temperature levels (see definition in Eq. (2)). Note that the stand-alone electrical power plant has the highest value of $\dot{W}_{net}$ but the lowest NPV and η_{ex}.

If we compare the rankings based on the TD optimization model results with those based on the TE optimization model results, there are some differences. In general, the TD results indicate the HB4 CHP as the best CHP layout. This is in line with results from previous work [7] and with the paper of Habka et al. [6]. Only for the 65/40 DH system at $\dot{Q}_{DH} = 20MWth$, the TD optimization results indicate the series CHP as the best configuration. However, from the TE optimization results it follows that the series CHP has almost always the best performance. Only for the connection to a 90/60 DH system at low heat demands, the HB4 CHP performs better. So from Table 6, we conclude that we cannot predict the optimal CHP configuration from the thermodynamic optimization results for all cases. The optimal CHP configuration can be indicated for half of the investigated cases. Only for the 90/60 DH system and a heat demand of 5MWth, the full ranking is correct.

The differences in the ranking between the TD and the TE optimized results are given by the bold values in the last two columns (for η_{ex}). For the 65/40 DH system at $\dot{Q}_{DH} = 5$ and $10MWth$, the TD optimization results predict an almost similar performance between the series and the HB4 set-ups. However, taking component sizes and economics into account, the difference between the series and the HB4 set-ups is more clear. In addition to the better performance of the series CHP, also the implementation is more simple. For the 65/40 DH system and $\dot{Q}_{DH} = 20MWth$, both models indicate the series CHP as the best configuration, however the second best set-up differs. The preheat-parallel configuration has the same performance as the series CHP based on the TD optimization results. However, when accounting for costs (TE results), its performance

		NPV [MEUR]	$\dot{W}_{net}$ [MWe]		η_{ex} [%]	
	$\dot{Q}_{DH}$ [MWth]	TE	TE	TD	TE	TD
65/40 DH system	5	1. S: 12.76	1. ORC: 3.38	1. ORC: 3.49	**1. S: 30.58**	**1. HB4: 31.81**
		2. HB4: 12.66	2. S: 3.33	2. HB4: 3.49	2. HB4: 30.53	2. S: 31.75
		3. PP: 11.65	3. HB4: 3.32	3. S: 3.48	3. PP: 28.82	3. PP: 31.75
		4. P: 11.14	4. PP: 3.10	4. PP: 3.48	4. P: 28.09	4. P: 28.93
		5. ORC: -2.81	5. P: 3.01	5. P: 3.12	5. ORC: 26.05	5. ORC: 26.89
	10	1. S: 28.41	1. ORC: 3.38	1. ORC: 3.49	**1. S: 35.24**	**1. HB4: 36.72**
		2. HB4: 28.09	2. S: 3.30	2. HB4: 3.49	2. HB4: 35.04	2. S: 36.66
		3. PP: 26.21	3. HB4: 3.27	3. S: 3.48	3. PP: 31.83	3. PP: 36.66
		4. P: 25.23	4. PP: 2.86	4. PP: 3.48	4. P: 30.26	4. P: 30.98
		5. ORC: -2.81	5. P: 2.65	5. P: 2.74	5. ORC: 26.05	5. ORC: 26.89
	20	1. S: 59.37	1. ORC: 3.38	1. ORC: 3.49	1. S: 43.81	1. S: 45.43
		2. HB4: 58.07	2. S: 3.14	2. S: 3.34	**2. HB4: 42.18**	**2. PP: 45.42**
		3. PP: 55.34	3. HB4: 2.93	3. PP: 3.34	3. PP: 37.55	3. HB4: 45.33
		4. P: 53.49	4. PP: 2.32	4. HB4: 3.33	4. P: 34.47	4. P: 35.06
		5. ORC: -2.81	5. P: 1.93	5. P: 2.00	5. ORC: 26.05	5. ORC: 26.89
90/60 DH system	5	1. HB4: 12.30	1. ORC: 3.38	1. ORC: 3.49	1. HB4: 32.21	1. HB4: 33.44
		2. PP: 11.03	2. HB4: 3.26	2. HB4: 3.42	2. PP: 29.69	2. PP: 30.55
		3. P: 10.60	3. PP: 2.93	3. PP: 3.04	3. P: 29.52	3. P: 30.23
		4. S: 10.50	4. P: 2.91	4. P: 3.00	4. S: 27.55	4. S: 27.36
		5. ORC: -2.81	5. S: 2.66	5. S: 2.63	5. ORC: 26.05	5. ORC: 26.89
	10	1. HB4: 27.25	1. ORC: 3.38	1. ORC: 3.49	1. HB4: 38.14	1. HB4: 40.53
		2. S: 25.85	2. HB4: 3.11	2. HB4: 3.42	**2. S: 34.42**	**2. PP: 34.61**
		3. PP: 25.27	3. S: 2.63	3. PP: 2.65	3. PP: 34.11	3. S: 34.45
		4. P: 24.16	4. PP: 2.59	4. S: 2.63	4. P: 32.88	4. P: 33.56
		5. ORC: -2.81	5. P: 2.43	5. P: 2.52	5. ORC: 26.05	5. ORC: 26.89
	20	1. S: 55.65	1. ORC: 3.38	1. ORC: 3.49	1. S: 46.41	1. HB4: 48.81
		2. HB4: 55.44	2. S: 2.35	2. HB4: 2.66	**2. HB4: 46.35**	**2. S: 47.66**
		3. PP: 53.69	3. HB4: 2.34	3. S: 2.51	3. PP: 43.55	3. PP: 47.65
		4. P: 51.45	4. PP: 1.98	4. PP: 2.51	4. P: 39.92	4. P: 40.23
		5. ORC: -2.81	5. P: 1.51	5. P: 1.54	5. ORC: 26.05	5. ORC: 26.89

Table 6: Ranking of the CHP configurations and the stand-alone electrical power plant based on the thermoeconomic (TE) and the thermodynamic (TD) optimization results. The net present value NPV, the net electrical power output $\dot{W}_{net}$ and the exergetic plant efficiency η_{ex} are considered. All configurations have a recuperated ORC.

is penalized due to the complexity and the higher number of components, and its performance is heavily worse than the series CHP for the TE optimized results. For the connection to the 90/60 DH system and $\dot{Q}_{DH} = 10MWth$, HB4 is correctly indicated as the best CHP but the potential of the preheat-parallel CHP is again overestimated by the TD model results. For a heat demand of $\dot{Q}_{DH} = 20MWth$, the HB4 configuration has better performance than the series CHP based on the TD optimization results, whereas the TE optimization model results show the opposite. However, the difference is small.

4. Conclusions

In this work, the thermoeconomic design optimization models for the series, parallel, preheat-parallel and HB4 combined heat-and-power (CHP) plant configurations are presented. The economic optimization of these four low-temperature geothermal CHP plant configurations is novel compared to the existing literature. The developed optimization framework can be used to indicate the most suitable CHP configuration and its optimal design for a certain district heating system connection and location.

We can conclude that the series configuration is generally the best for the connection to a low-temperature district heating system and for a high-temperature district heating system with high heat demands. For the connection to a high-temperature district heating system with lower heat demands, the HB4 configuration performs better. Furthermore, we have found that the CHP plants are economically more attractive than a stand-alone electrical power plant, and that the net present value increases from -2.81MEUR for the stand-alone electrical power plant to approximately $12.5MEUR$, $28MEUR$ and $58MEUR$ for a CHP plant with a heat delivery of 5, 10 and 20MWth, respectively, and under the assumptions considered. So by producing heat next to electricity, the geothermal project turns into a profitable project. Also, the exergetic plant efficiency might be up to 20.36%-pts higher than for the stand-alone electrical power plant, which indicates a better utilization of the low-temperature geothermal energy source in a CHP plant. However, the net electrical power production might be up to 30% lower than for a stand-alone electrical power plant.

Furthermore, we want to emphasize the importance of including economics in the optimization.

First, the cooling cost of a low-temperature geothermal (combined heat-and-)power plant is very important ($\sim 70\%$ of the total ORC cost) and has a strong impact on the condenser temperature. This explains why the condenser temperature is typically higher when economics are included compared to a thermodynamic analysis. As a result, the electricity production which is calculated in a thermodynamic analysis is generally overestimated. And second, the geometry of the heat exchangers and the air-cooled condenser should be modeled to allow proper heat transfer, pressure drop and cost calculations. That way, a number of strong assumptions (pinch-point-temperature differences, condenser temperature, pressure drops, ...) which are typical for a thermodynamic cycle analysis can be eliminated, and they are optimized by the thermoeconomic optimization model.

Finally, we conclude that the net present value is a better optimization objective than the electricity production since the decision whether or not to invest in a (geothermal) project is based on economics rather than thermodynamics.

Acknowledgments

This project receives the support of the VITO PhD grant number 1510829.

Nomenclature

Abbreviations

symbol	description
ACC	air-cooled condenser
CHP	combined heat-and-power
DH	district heating system
ECO	economizer
EVAP	evaporator
GWP	global warming potential
ODP	ozone depletion potential
ORC	organic Rankine cycle
RECUP	recuperator
SUP	superheater

Symbols

symbol	description
B_c [m]	baffle cut
D_{shell} [m]	shell diameter
D_{tube} [mm]	tube diameter
d_{el} [%]	yearly electricity price increase
dr [%]	discount rate
$\dot{E}$ [MW]	flow exergy
ex [kJ/kg]	specific flow exergy
H_{fin} [mm]	heigh of fin ACC
h [kJ/kg]	specific enthalpy
I [MEUR]	investment costs
L [years]	lifetime
L_{bc} [m]	length between baffles
$\dot{m}$ [kg/s]	mass flow rate
N	availability factor
NPV [MEUR]	net present value
n_{tube}	number of tubes ACC
p [bar]	pressure
p_{el} [EUR/MWh]	electricity price
p_{heat} [EUR/MWh]	heat price
p_{tube} [mm]	tube pitch
$\dot{Q}$ [MWth]	heat
S_{fin} [mm]	spacing between fins ACC
s [kJ/kgK]	specific entropy
T [$^{\circ}C$]	temperature
$\dot{W}$ [MWe]	electrical power
ϵ [%]	recuperator efficiency
η [%]	efficiency

Subscripts & superscripts

symbol	description
1	condenser state
4	evaporator state
6	turbine inlet state
b	brine
$cond$	condenser
cw	cooling water
$crit$	critical point
en	energetic
env	environment
ex	exergetic
f	fan
g	generator
inj	injection state
m	motor
mid	intermediate state DH water
min	minimum
net	net
out	outlet
p	pump
$prod$	production state
$return$	return state DH system
sup	superheating
$supply$	supply state DH system
t	turbine
$upper$	upper limit by REFPROP
$wells$	wells
wf	working fluid

References

[1] S. Van Erdeweghe, J. Van Bael, B. Laenen, W. D'haeseleer, Design and off-design optimization procedure for low-temperature geothermal organic Rankine cycles, Applied Energy 242 (2019) 716–731.

[2] F. Heberle, D. Brüggemann, Exergy based fluid selection for a geothermal Organic Rankine Cycle for combined heat and power generation, Applied Thermal Engineering 30 (2010) 1326–1332.

[3] M. Habka, S. Ajib, Determination and evaluation of the operation characteristics for two configurations of combined heat and power systems depending on the heating plant parameters in low-temperature geothermal applications, Energy Conversion and Management 76 (2013) 996–1008.

[4] M. Habka, S. Ajib, Studying effect of heating plant parameters on performances of a geothermal-fuelled series cogeneration plant based on Organic Rankine Cycle, Energy Conversion and Management 78 (2014) 324–337.

[5] S. Van Erdeweghe, J. Van Bael, B. Laenen, W. D'haeseleer, Comparison of series/parallel configuration for a low-T geothermal CHP plant, coupled to thermal networks, Renewable Energy 111 (2017) 494–505.

[6] M. Habka, S. Ajib, Investigation of novel, hybrid, geothermal-energized cogeneration plants based on organic Rankine cycle, Energy 70 (2014) 212–222.

[7] S. Van Erdeweghe, J. Van Bael, B. Laenen, W. D'haeseleer, Optimal combined heat-and-power plant for a low-temperature geothermal source, Energy 150 (2018) 396–409.

[8] F. Marty, S. Serra, S. Sochard, J.-M. Reneaume, Simultaneous optimization of the district heating network topology and the Organic Rankine Cycle sizing of a geothermal plant, Energy 159 (2018) 1060–1074.

[9] S. Van Erdeweghe, J. Van Bael, B. Laenen, W. D'haeseleer, Preheat-parallel configuration for low-temperature geothermally-fed CHP plants, Energy Conversion and Management 142 (2017) 117–126.

[10] O. A. Oyewunmi, C. J. Kirmse, A. M. Pantaleo, C. N. Markides, Performance of working-fluid mixtures in ORC-CHP systems for different heat-demand segments and heat-recovery temperature levels, Energy Conversion and Management 148 (2017) 1508–1524.

[11] C. Wieland, D. Meinel, S. Eyerer, H. Spliethoff, Innovative CHP concept for ORC and its benefit compared to conventional concepts, Applied Energy 183 (2016) 478–490.

[12] D. Fiaschi, A. Lifshitz, G. Manfrida, D. Tempesti, An innovative ORC power plant layout for heat and power generation from medium- to low-temperature geothermal resources, Energy Conversion and Management 88 (2014) 883–893.

[13] S. Bos, B. Laenen, Development of the first deep geothermal doublet in the Campine Basin of Belgium, European Geologist 43 (2017) 16–20.

[14] Informationsportal Tiefe Geothermie, Grünwald, 2018. URL: https://www.tiefegeothermie.de/projekte/gruenwald.

[15] The Dark Sky Company, Dark Sky API, 2012. URL: www.darksky.net.

[16] P. Garg, M. S. Orosz, P. Kumar, Thermo-economic evaluation of ORCs for various working fluids, Applied Thermal Engineering 109 (2016) 841–853.

[17] J. Calm, G. Hourahan, Physical, Safety and Environmental Data for Current and Alternative Refrigerants, in: International Congress of Refrigeration, Prague, Czech Republic, 2011. URL: http://www.hourahan.com/wp/wp-content/uploads/2010/08/2011-Physical-Safety-and-Environmental-Data2.pdf.

[18] D. Walraven, B. Laenen, W. D'haeseleer, Optimum configuration of shell-and-tube heat exchangers for the use in low-temperature organic Rankine cycles, Energy Conversion and Management 83 (2014) 177–187.

[19] L. Yang, H. Tan, X. Du, Y. Yang, Thermal-flow characteristics of the new wave-finned flat tube bundles in air-cooled condensers, International Journal of Thermal Sciences 53 (2012) 166–174.

[20] R. Bertani, Perspectives for Geothermal Energy in Europe, World Scientific (Europe), 2017. URL: http://www.worldscientific.com/worldscibooks/10.1142/q0069. doi:10.1142/q0069.

[21] G. Manente, L. Da Lio, A. Lazzaretto, Influence of axial turbine efficiency maps on the performance of subcritical and supercritical Organic Rankine Cycle systems, Energy 107 (2016) 761–772.

[22] IEA, Technology Roadmap - Geothermal Heat and Power, 2011. URL: https://www.iea.org/newsroomandevents/pressreleases/2011/june/how-to-achieve-at-least-a-tenfold-increase-in-supply-of-geothermal-power-and-hea.html.

[23] TEMA, Standards of the tubular exchanger manufacturers association, 1999. URL: http://www.funke.de/pdf/zertifikate/tema.pdf.

[24] G. van Rossum, Python Tutorial, Technical Report CS-R9526, Technical Report, Centrum voor Wiskunde en Informatica (CWI), Amsterdam, 1995. URL: http://www.python.org.

[25] J. Andersson, A General-Purpose Software Framework for Dynamic Optimization, Phd, Arenberg Doctoral School, KU Leuven, 2013. URL: https://lirias2repo.kuleuven.be/bitstream/id/243411/.

[26] A. Wächter, L. T. Biegler, On the implementation of an interior-point filter line-search algorithm for large-scale nonlinear programming, Mathematical Programming 106 (2006) 25–57.

[27] E. Lemmon, M. Huber, M. McLinden, REFPROP - Reference Fluid Thermodynamic and Transport Properties. NIST Standard Reference Database 23, 2007.